Photovoltaic properties of anisotropic relaxation semiconductors

J. F. Schetzina
Department of Physics, North Carolina State University, Raleigh, North Carolina 27607
(Received 23 June 1975)

A relaxation-case theory for the photovoltaic effect which occurs in anisotropic semiconductors is developed. Expressions for the short-circuit photocurrent and open-circuit photovoltage, valid for linear conductivity-locked transport, are obtained for the case of constant (depth-independent) conductivity anisotropy. These show that anisotropic relaxation semiconductors can generate large open-circuit photovoltages in some cases. A material in which the anisotropy factor a varies with depth is also considered and several specific cases are analyzed in detail. The properties of a new photovoltaic structure, an isojunction, emerge from this analysis. The isojunction, a structure composed of two different regions characterized by anisotropy factors of opposite sign and containing an isoplane at which $a = 0$, possesses certain new and novel properties. This structure can, for example, generate photovoltages of opposite polarity when illuminated with light of different wavelengths. A new theory for the widely observed larger-than-bandgap "anomalous" photovoltages exhibited by many obliquely deposited polycrystalline semiconducting films is proposed. The theory is obtained by considering this class of photovoltaic films to be examples of anisotropic relaxation semiconductors. In a simple and self-consistent way, the new theory accounts in detail for the various aspects of observed behavior and yields good numerical estimates of photovoltages and photocurrents when relaxation-case values for parameters of the theory are employed.

I. INTRODUCTION

van Roosbroeck has provided a new approach to understanding electronic transport in amorphous semiconductors by introducing[1] the concept of the relaxation semiconductor and describing[1,2] many of its interesting properties. In addition, van Roosbroeck and co-workers have analyzed[3-5] some aspects of transport in crystalline relaxation semiconductors as well. These papers are concerned with materials in which $\tau < \tau_d$, where τ is the carrier lifetime and τ_d is the dielectric relaxation time, whereas the lifetime semiconductor with $\tau > \tau_d$ is the familiar type.

A principal result of the nonlinear large-signal analysis is recombinative space-charge injection. Through single-carrier injection, a condition of quasizero net recombination rate $R \approx 0$ can be achieved on a local basis. Injection of minority carriers into a relaxation semiconductor can accordingly lead to a substantial local depletion of majority carriers since, in the region in which it holds, the condition $R \approx 0$ implies that the product of electron and hole concentrations is approximately equal to its thermal equilibrium value ($np \approx n_0 p_0$). On the basis of normalized continuity equations solved by numerical procedures it has recently been shown[6] that the predicted van Roosbroeck depletion of majority carriers does indeed occur for sufficiently large injection currents and whenever $\tau < \tau_d$. In contrast to the lifetime case, the computed characteristics for a pronounced relaxation semiconductor show an extended region of injected space charge characterized by $R \approx 0$ which terminates at a narrow recombination front ($np \gg n_0 p_0$) where injected minority carriers recombine with majority carriers.[6]

van Roosbroeck has proposed a model[2] which is based on the general properties of the relaxation semiconductor to account for the widely observed switching effects exhibited by many amorphous semiconductor alloys. This model, in a self-consistent way, accounts for the various properties which these materials display including a small negative Hall coefficient, a positive Seebeck coefficient, preswitching behavior, threshold switching, the "blocked ON state," and the field effect. The detailed agreement with experimental observations provides the strongest evidence that this model is essentially correct.

Optical injection in relaxation semiconductors, a process that introduces both types of carriers, is the subject of a recent paper[7] which suggests that under certain conditions such injection can lead to a simple but particular type of steady-state transport. In cases where carrier lifetimes are not significantly altered by the illumination, the steady-state conductivity ratio $K = \sigma_n / \sigma_p$ remains essentially constant and a linear *conductivity-locked* mode of transport can occur. On the basis of this condition, a theory[7] for the Hall effect, photoconductivity, the Dember effect, and the photomagnetoelectric effect was developed. This paper enlarges upon the above presentation and analyzes in detail a new aspect of relaxation-regime transport. In Sec. II, an illuminated *anisotropic* trap-dominated relaxation semiconductor is considered. The discussion is thus limited to crystalline relaxation

semiconductors.

When the surface of an anisotropic semiconductor is illuminated with light, a carrier concentration gradient forms normal to the surface and this is accompanied by the diffusion of photogenerated carriers into the bulk. As a consequency of anisotropy, however, the diffusion of electrons may proceed in a direction different from that of holes. In this case, a photovoltaic effect occurs. A detailed analysis of this effect in lifetime semiconductors is available in the literature.[8-10] Here, a relaxation-case theory is developed. In Sec. II, expressions for the short-circuit current I_{sc} and open-circuit photovoltage per unit length V_{oc}, valid for linear conductivity-locked transport, are obtained for the case of constant (depth-independent) conductivity anisotropy. These expressions show that anisotropic relaxation semiconductors can generate large open-circuit photovoltages in some cases.

A semiconductor in which the anisotropy factor a varies with depth is also considered and several specific variations are treated in detail. The properties of a new photovoltaic structure, an *isojunction*, emerge from this analysis. The isojunction, a structure composed of two different anisotropic regions characterized by anisotropy factors of opposite sign and containing an *isoplane* at which $a=0$, possesses certain new and novel properties which are pointed out in Sec. II. The extension of the theory to include anisotropic structures of increased complexity is also discussed.

The widely observed larger-than-band-gap "anomalous" photovoltages exhibited by many obliquely deposited polycrystalline semiconductor films are discussed in Sec. III. A new theory for this effect is presented here. The theory is obtained by considering this class of photovoltaic films to be examples of anisotropic trap-dominated relaxation semiconductors. In a simple and self-consistent way, the new model accounts in detail for the various aspects of observed behavior. Properties treated include, for example, the typically high resistivity which the photovoltaic films display; the variation in short-circuit current and open-circuit photovoltage with illumination intensity; the saturation in open-circuit photovoltages at illumination levels which vary in reverse order of band-gap energies; the vastly different photovoltaic spectral sensitivities which films of a given semiconductor exhibit; the one-to-one correspondence between open-circuit photovoltage and film resistance that is observed in some cases; the effect of through-the-substrate illumination on photovoltaic properties; the giant photomagnetoelectric effect in CdTe films; the switching effects observed in polycrystalline CdTe films and their implications.

II. THEORY

A. Conductivity-locked transport in trap-dominated relaxation semiconductors

In a lifetime semiconductor with negligible trapping, excess carrier transport is *number-density locked*. That is, the density δn of excess electrons is everywhere equal to the density δp of excess holes. The ratio $\delta n/\delta p = 1$ is controlled by fast dielectric relaxation processes which characterize the lifetime regime and the distribution of excess carriers can accordingly be treated as a quasineutral plasma. This quasineutral plasma never forms in a relaxation semiconductor. With $\tau < \tau_d$, the carriers recombine before it can be established. In cases involving steady optical injection of carriers, however, an approximate state of *overall* neutrality is maintained by fast *equality recombination*, that is, recombination of electrons and holes at equal volume capture rates.[2]

Conductivity-locked transport will occur in trap-dominated relaxation semiconductors provided the densities of neutral and charged equality centers which control the recombination rate are not significantly altered by the incident radiation. Such a condition can prevail in a strongly trap-dominated material even though appreciable modulation in free-carrier densities may have occurred. Consider, for example, the simplest case of a p-type relaxation semiconductor with large concentrations of deep donors and acceptors. In this case, for a mobility ratio $\mu_n/\mu_p > 1$, a recombination asymmetry will prevail with nearly all of the recombination events occurring at the acceptor centers. Under steady illumination and for acceptors at a single energy level, the electron and hole capture times may be expressed as

$$\tau_{tn} = [C_n(N-\hat{n})]^{-1}, \quad \tau_{tp} = (C_p\hat{n})^{-1}, \tag{1}$$

respectively. In the above expressions, C_n and C_p are electron and hole capture coefficients, N is the total density of acceptors, and $\hat{n}$ is the density of charged acceptors. The steady-state nonequilibrium recombination rate in this case is given by

$$\begin{aligned} \mathcal{R} &= C_n[n(N-\hat{n}) - n_1\hat{n}] = \delta n/\tau_n, \\ &= C_p[p\hat{n} - p_1(N-\hat{n})] = \delta p/\tau_p. \end{aligned} \tag{2}$$

In (2), n and p are electron and hole concentrations, n_1 and p_1 are the corresponding mobile carrier concentrations with the Fermi level at the energy level of the acceptors, and δn and δp are concentrations of excess electrons and holes, characterized by lifetimes τ_n and τ_p, respectively. In obtaining (2), direct electron-hole recombination as well as recombination at the donor centers has been neglected.

Now, a trap-dominated relaxation semiconductor

is defined[2,7] such that $N-\hat{n}_0 \gg \hat{n}_0 \gg n_0, p_0$, where the zero subscripts indicate equilibrium values. Then, provided $\hat{n}_0 \gg n, p$ is maintained under illumination, charge neutrality implies $\hat{n} \approx \hat{n}_0$ and $N-\hat{n} \approx N-\hat{n}_0$. That is, under such conditions the illumination does not significantly change the carrier capture times from their equilibrium values even though appreciable mobile carrier modulation ($n, p \gg n_0, p_0$) may have occurred. It then follows from (2) that the excess electron and hole lifetimes are unequal and constant, being governed by the rate of capture of the respective carriers by the equality centers. That is,

$$\tau_n = \tau_{tn} = [C_n(N-\hat{n}_0)]^{-1}, \quad \tau_p = \tau_{tp} = (C_p \hat{n}_0)^{-1}. \tag{3}$$

A similar argument can be made for recombination involving equality centers at more than one energy level and also for recombination at donor centers. In all of these cases, carrier lifetimes that are unequal and essentially independent of the illumination level result.[11,12]

Equality recombination, or recombination at equal volume capture rates, means $n/\tau_{tn} = p/\tau_{tp}$ and thus the conductivity ratio may be expressed as

$$K = \sigma_n/\sigma_p = \mu_n \tau_{tn}/(\mu_p \tau_{tp}), \tag{4}$$

where μ_n and μ_p are electron and hole mobilities, respectively. The concept of conductivity-locked transport follows immediately from (4) for constant carrier mobilities and capture times.

Carrier mobilities may be expressed as

$$\mu_n = e\tau_{fn}/m_n^* = eL_{fn}/(3kTm_n^*)^{1/2},$$
$$\mu_p = e\tau_{fp}/m_p^* = eL_{fp}/(3kTm_p^*)^{1/2}, \tag{5}$$

where τ_f, L_f, and m^* are the mean scattering time, mean free path, and effective mass, respectively. Single-free-path recombination in strongly trap-dominated relaxation semiconductors means

$$\tau_{fn} = \tau_{tn}, \quad \tau_{fp} = \tau_{tp}. \tag{6}$$

Using (4)–(6), the conductivity ratio may then be expressed as

$$K = (L_{fn}/L_{fp})^2 \tag{7}$$

for this type of recombination. Equal-free-path equality recombination thus produces the $K=1$ or minimum conductivity state of the relaxation regime, as has been pointed out by van Roosbroeck.[2] States other than $K=1$ occur for materials which exhibit single-free-path recombination when carrier mean free paths are unequal. In the absence of single-free-path recombination, the more general expression (4) applies and determines the conductivity ratio.

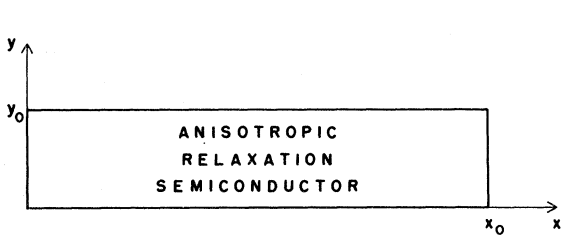

FIG. 1. Geometry of specimen considered in text.

B. Illuminated anisotropic relaxation semiconductor

Let us consider an anisotropic relaxation semiconductor as shown in Fig. 1 having dimensions x_0, y_0 and unit width along z with the lower surface at $y=0$ subjected to steady uniform illumination. We assume the semiconductor to be characterized by hole and electron conductivity tensors $\overleftrightarrow{\sigma}_p$ and $\overleftrightarrow{\sigma}_n$ that are anisotropic in the xy plane and whose principal axes do not coincide with the x and y axes of the specimen. For small conductivity anisotropies, such tensors may be expressed in matrix form in the specimen coordinate system as

$$\overleftrightarrow{\sigma}_p = \sigma_p \begin{pmatrix} 1 & a_p & 0 \\ a_p^* & 1 & 0 \\ 0 & 0 & 1 \end{pmatrix}, \quad \overleftrightarrow{\sigma}_n = \sigma_n \begin{pmatrix} 1 & a_n & 0 \\ a_n^* & 1 & 0 \\ 0 & 0 & 1 \end{pmatrix}. \tag{8}$$

In (8), $a_p = \sigma_{pxy}/\sigma_p$, $a_p^* = \sigma_{pyx}/\sigma_p$, $a_n = \sigma_{nxy}/\sigma_n$, and $a_n^* = \sigma_{nyx}/\sigma_n$ are dimensionless hole and electron anisotropy factors. They are zero for an isotropic semiconductor. Carrier mobility tensors are

$$\overleftrightarrow{\mu}_p = \overleftrightarrow{\sigma}_p/pe, \quad \overleftrightarrow{\mu}_n = \overleftrightarrow{\sigma}_n/ne, \tag{9}$$

where p and n are hole and electron concentrations, respectively, and e is the (positive) electronic charge. With Boltzmann statistics, the corresponding diffusivities are

$$\overleftrightarrow{D}_p = (kT/e)\overleftrightarrow{\mu}_p, \quad \overleftrightarrow{D}_n = (kT/e)\overleftrightarrow{\mu}_n, \tag{10}$$

where k is the Boltzmann constant and T is the absolute temperature.

We seek expressions for the short-circuit current I_{sc} and open-circuit photovoltage per unit length V_{oc}. It will be assumed that the specimen is sufficiently trap dominated such that transport in the steady state is conductivity locked. Let us first consider the case of constant (depth-independent) conductivity anisotropy. To first order in anisotropy factors, this case is the phenomenological equivalent of the photomagnetoelectric (PME) effect[13] which is analyzed in detail in Ref. 7. Here we list only the principal results of this analysis. For the geometry considered, the distribution of photogenerated holes within the semiconductor is given by[7]

$$\delta p = \delta p_0^*(C_1 e^{-Y} + C_2 e^{Y} + e^{-AY}), \tag{11}$$

where

$$\delta p_0^* = \alpha\beta\tau_p I_0/(1-A^2)\,. \tag{12}$$

The corresponding distribution of photogenerated electrons is simply $\delta n = (\tau_n/\tau_p)\delta p$. The short-circuit current and open-circuit photovoltage per unit length may be expressed as[7]

$$I_{sc} = -eD_p^* \int_0^{Y_0} a\left(\frac{d\delta p}{dY}\right) dY\,, \tag{13}$$

$$V_{oc} = \frac{-eD_p^* \int_0^{Y_0} a(d\delta p/dY)\,dY}{(1+K)L^* \int_0^{Y_0} \sigma_p\, dY}\,, \tag{14}$$

respectively. Using (11), the above expressions reduce to

$$I_{sc} = J^* L^*\,, \tag{15}$$

$$V_{oc} = J^*/(\sigma_0 Y_0 + \Sigma_0^*)\,. \tag{16}$$

In (11)–(16), I_0 is the illumination intensity at the $y=0$ surface after reflection losses, α is the absorption coefficient, β is the quantum efficiency for electron-hole pair creation, σ_0 is the equilibrium conductivity, and $K=\sigma_n/\sigma_p$ is the conductivity ratio. Also, $L^* = (D_p^*\tau_p)^{1/2} \equiv (D_n^*\tau_n)^{1/2}$ is a conductivity-locked diffusion length, with

$$\begin{aligned} D_p^* &= (kT/e)[2K/(1+K)]\,\mu_p\,, \\ D_n^* &= (kT/e)[2/(1+K)]\,\mu_n\,. \end{aligned} \tag{17}$$

$A=\alpha L^*$ is a dimensionless absorption coefficient, $Y=y/L^*$ is a dimensionless length, and $a=a_p-a_n$. In addition, in (15) and (16), $J^*=aJ_0^*$ is a current density for which

$$J_0^* = [e\beta A I_0/(1-A^2)]\,[C_1(1-e^{-Y_0}) + C_2(1-e^{Y_0}) + (1-e^{-AY_0})]\,, \tag{18}$$

and Σ_0^* is a photoconductivity given by

$$\Sigma_0^* = \frac{(1+K)^2}{2K}\,\frac{e^2\beta A L^* I_0}{kT(1-A^2)} \times\left(C_1(1-e^{-Y_0}) + C_2(e^{Y_0}-1) + \frac{1-e^{-AY_0}}{A}\right). \tag{19}$$

In the above expressions

$$\begin{aligned} C_1 &= -\frac{(S_1+A)(S_2+1)\,e^{Y_0} - (S_2-A)(S_1-1)\,e^{-AY_0}}{2(S_1S_2+1)\sinh Y_0 + 2(S_1+S_2)\cosh Y_0}\,, \\ C_2 &= \frac{(S_1+A)(S_2-1)\,e^{-Y_0} - (S_2-A)(S_1+1)\,e^{-AY_0}}{2(S_1S_2+1)\sinh Y_0 + 2(S_1+S_2)\cosh Y_0}\,, \end{aligned} \tag{20}$$

where S_1 and S_2 are dimensionless surface recombination velocities, or *surface numbers*, at the illuminated and dark surfaces, respectively. These surface numbers are defined as

$$S = s_p L^*/D_p^* \equiv s_n L^*/D_n^*\,, \tag{21}$$

where s_p and s_n are surface recombination velocities for holes and electrons, respectively. For a strongly trap-dominated relaxation semiconductor, surface numbers of order one are to be expected. $S=1$ corresponds physically to a carrier surface recombination velocity s_p, s_n equal to the respective bulk diffusion velocity $v_p = D_p^*/L^*$, $v_n = D_n^*/L^*$. The surfaces of a $K=1$ state amorphous semiconductor, for example, might well be characterized by $S\approx 1$ since in this case the surfaces are not appreciably different from the bulk.

Note, in particular, that (15) expresses a short-circuit current I_{sc} which is directly proportional to the illumination intensity I_0. For small light intensities, the open-circuit photovoltage V_{oc} given by (16) reduces to

$$V_{oc} = R_0 I_{sc}\ (\text{small } I_0)\,, \tag{22}$$

where R_0 is the specimen electrical resistance per unit length in the absence of added carriers. At large illumination levels, (16) reduces to

$$V_{oc} = J^*/\Sigma_0^*\ (\text{large } I_0)\,. \tag{23}$$

Thus, the photovoltage saturates and is independent of I_0 in this limit.

Note also that for the small conductivity-locked diffusion lengths which are expected for a trap-dominated relaxation semiconductor ($L^* \approx 10^{-4}$–10^{-6} cm), short-circuit currents will also be small. Large open-circuit photovoltages may result, however, since Σ_0^* in (23) contains L^* as a factor. These important properties of anisotropic relaxation semiconductors will be discussed in greater detail in Sec. III.

Other types of conductivity anisotropies can also be analyzed. Consider, for example, a material in which the anisotropy factor varies with depth. In this case, the hole continuity equation may be expressed as

$$\frac{d^2\delta p}{dY^2} - \frac{eL^*E_x}{2kT}\,\frac{d(a^*p)}{dY} - \delta p + \alpha\beta I_0\tau_p e^{-AY} = 0\,, \tag{24}$$

where $a^* = a_p^* - a_n^*$. The drift term in (24) takes into account the presence of the internal field E_x which results from the anisotropic diffusion. This term is zero, of course, under short-circuit conditions since $E_x=0$. Its inclusion in (24) and in the boundary conditions[7] yields a modified carrier distribution which leads to a transcendental equation for V_{oc}. However, for small anisotropy factors and short conductivity-locked diffusion lengths, these solutions reduce to (11) and (16), respectively. Further formulation will accordingly employ the carrier distribution (11).

Let us consider a structure in which the anisotropy factor a varies linearly with depth [Fig. 2(a)]. In this case the anisotropy factor may be expressed as

$$a(Y) = [(a_2-a_1)/Y_0]\,Y + a_1\,, \tag{25}$$

where a_1 and a_2 are the values of a at the illuminated ($Y=0$) and dark ($Y=Y_0$) surfaces, respec-

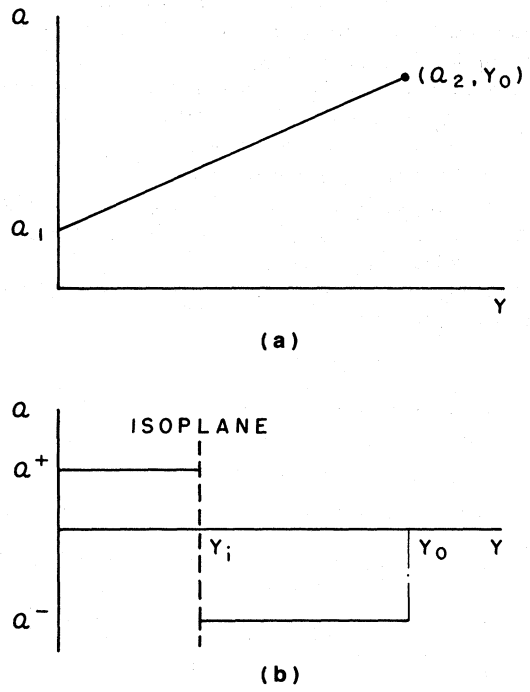

FIG. 2. Anisotropy factors for (a) structure in which conductivity anisotropy varies linearly with depth, (b) an abrupt a^+-a^- isojunction.

tively. Solutions for the short-circuit current and open-circuit photovoltage per unit length are readily obtained using (11), (13), and (14). These solutions are given by (15) and (16), respectively, in which

$$J^* = \frac{e\beta A I_0}{1-A^2}\{a_1(C_1+C_2+1) - a_2(C_1 e^{-Y_0} + C_2 e^{Y_0} + e^{-AY_0}) + [(a_2-a_1)/Y_0][C_1(1-e^{-Y_0}) + C_2(e^{Y_0}-1) + (1-e^{-AY_0})/A]\} . \quad (26)$$

Next, consider a structure in which the anisotropy factor changes sign, say, from a positive value at the illuminated ($Y=0$) surface to a negative value at some depth. There will then be a plane of isotropy, an *isoplane*, at some $Y=Y_i$ which defines the junction of these two different regions. Let us call this structure which contains an isotropic junction plane, an *isojunction*. The anisotropy factor associated with an abrupt a^+-a^- isojunction is shown in Fig. 2(b). The above labeling scheme gives the sign of the anisotropy factor in the order seen by a light beam as it passes through the structure.

An illuminated isojunction produces a transverse electric field and thus a photovoltage directly proportional to its length. An isojunction has a basic asymmetry which primarily depends on the relative magnitudes of a^+ and a^- and on the depth of its isoplane. Because of this fundamental asymmetry, an isojunction can generate photovoltages of opposite polarity when illuminated with light of different absorption characteristics. In addition, its spectral sensitivity to radiation may be entirely different when the direction of illumination is reversed. Corresponding changes in the direction of short-circuit current flow will also result under these conditions. These novel properties of an isojunction are shown schematically in Fig. 3. Here, an abrupt a^+-a^- isojunction is illustrated.

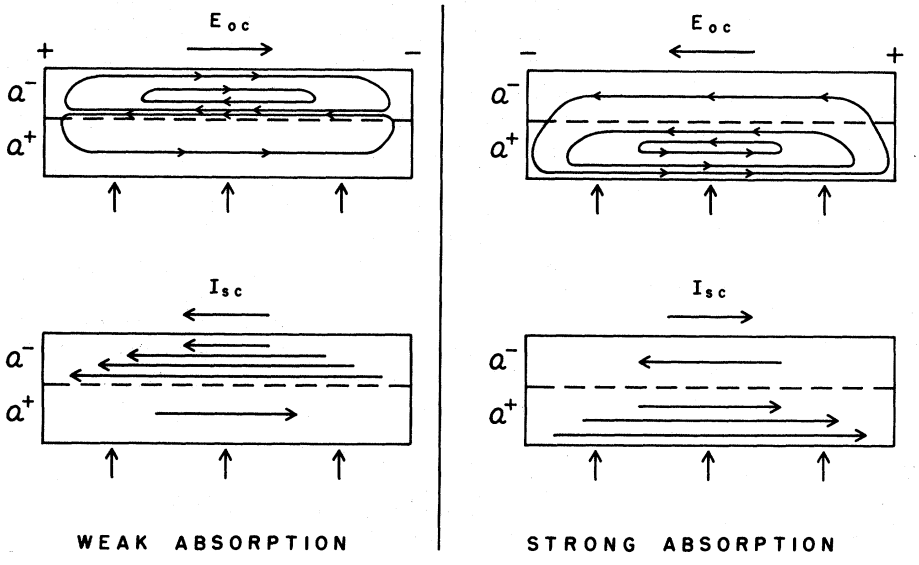

FIG. 3. The illuminated isojunction: Short-circuit currents I_{sc} and open-circuit fields E_{oc} are shown qualitatively for cases of weak and strong absorption of light. Different open-circuit circulating current densities develop in these limits as shown.

Open-circuit and short-circuit current densities are shown qualitatively for cases of weak and strong absorption of light, respectively. In the strong absorption limit, illustrated behavior is similar to that which occurs in the photomagnetoelectric effect.[13] The isojunction produces a transverse open-circuit field E_{oc} of indicated polarity and an open-circuit circulating current density results. Near the illuminated surface of the a^+ region, this current density is due mainly to the anisotropic diffusion of photogenerated electrons and holes and flows to the right as shown. Deeper within the bulk, drift in the presence of the internal field E_{oc} dominates and the current density reverses direction. Under short-circuit conditions, the transverse field is zero and a net current I_{sc} flows to the right as indicated. In the weak absorption limit and with $a^- > a^+$ in magnitude, a polarity reversal in E_{oc} occurs and a twin-looped open-circuit circulating current density develops. Net short-circuit current flow is to the left as shown. Illustrated behavior does not include surface effects, however, which can be significant in some cases. Because of its fundamental asymmetry, the photovoltaic spectral sensitivity of the isojunction shown in Fig. 3 will be entirely different when the direction of illumination is reversed. For a given source of radiation, short-circuit currents and open-circuit photovoltages of different magnitudes and/or polarities may be produced in this case.

The properties of an abrupt a^+-a^- isojunction may be analyzed using (11), (13), and (14). Solutions for the short-circuit current and open-circuit photovoltage per unit length are easily obtained and are given by (15) and (16), respectively, with

$$J^* = [e\beta A I_0/(1-A^2)][a^+(C_1+C_2+1) - a^-(C_1 e^{-Y_0} + C_2 e^{Y_0} + e^{-AY_0}) - (a^+ - a^-)(C_1 e^{-Y_i} + C_2 e^{Y_i} + e^{-AY_i})] \quad (27)$$

for this type of structure. In the above expression, Y_i is the (dimensionless) depth of the isoplane from the illuminated ($Y=0$) surface.

An abrupt isojunction is, of course, an idealization. The abrupt change in the anisotropy factor associated with this structure leads to a singularity in the drift term of (24) at the junction plane. In reality, however, this change would ordinarily occur over some finite distance. Accordingly, the above analysis employs the more realistic diffusive carrier distribution (11) in the integrations specified by (13) and (14) but assumes constant anisotropy factors in the two separate regions. That is, the variation in the anisotropy factor *near* the junction plane is neglected.

The properties of a linearly graded a^+-a^- isojunction can also be analyzed. In this case, the appropriate J^* is obtained by setting $a_1 = a^+$ and $a_2 = a^-$ in (26). With this J^*, (15) and (16) give I_{sc} and V_{oc}, respectively. In this way, a hierarchy of increasingly complex anisotropic structures, such as an a^+-a^--a^+ double isostructure, can be defined and treated.

We would like to suggest a method which could be used to produce semiconducting structures of the type described above. Two principal conditions must be met for the present analysis to be applicable: The semiconducting material must be characterized by conductivity tensors of the form given by (8) and it must be sufficiently trap dominated so that the transport is conductivity locked. It would seem that the preparation of polycrystalline films of appropriate semiconductors by means of an *oblique*-vapor-deposition process could satisfy both of these requirements. Such a process might induce nontypical crystal growth with close-packed planes gradually tilting toward the vapor-deposition direction and hence produce crystals having the required anisotropy. In addition, such nontypical growth might be accompanied by appreciable densities of impurity and/or disorder-induced localized electronic states. The material would then be an anisotropic trap-dominated relaxation semiconductor and should exhibit an extraordinary photovoltaic effect. Obliquely deposited semiconducting films have, of course, been widely studied for many years. When illuminated, these films produce large "anomalous" photovoltages.

III. ANOMALOUS PHOTOVOLTAIC EFFECT

A. History

Semiconducting thin films which generate larger-than-band-gap photovoltages have been the subject of numerous investigations.[14–54] The effect has been observed in many semiconductors including CdTe,[14–16] Ge,[17,18] Si,[17,27] GaAs,[19] GaP,[20] ZnTe,[21] PbI_2,[22] Sb_2S_3,[23,24] and Sb_2Se_3,[25] when films of these materials are prepared using an oblique-vapor-deposition technique. Films prepared with the vapor flow normal to the substrate produce little or no photovoltages. In cases where determined, the photovoltaic films are found to be polycrystalline and often display surfaces of a textured nature.

The history of these photovoltaic films is somewhat bizarre, with the literature filled with many seemingly contradictory observations. Different researchers report photovoltages of opposite polarity for films of a given semiconductor.[16,17,25,50,51] Some films are found to be quite sensitive to radiation of near-band-gap frequency,[19–22] while others display a spectral sensitivity that increases monotonically with photon energy.[19,20,26] Still others exhibit short-circuit cur-

rents and open-circuit photovoltages of different polarity in some regions of the spectrum.[24,31] Illumination of the films through the substrate quite typically leads to an entirely different photovoltaic response.[29,30] Some of the films exhibit photovoltages of opposite polarity in this case, while others do not. Some specimens generate photovoltages of hundreds of volts per centimeter film length when exposed to intense white light.[16,19] Others, prepared under nearly identical conditions, show little or no photovoltaic properties. Because of the above observations, the photovoltaic effect which these semiconducting films display has come to be called the "anomalous" photovoltaic effect.

Several theoretical models have been proposed, each of which explains certain aspects of the effect. However, none of these models can account for all of the experimental observations. It is generally believed that the generation of large potential differences along the length of these thin films must result from the addition of voltages from a series arrangement of some kind of microelements. Electron-microscopic studies[47,52] of obliquely deposited CdTe show that these films are composed of small, obliquely oriented crystallites 100–200 nm in size. These individual crystallites may be the microelements involved. Two distinct types of models have been proposed which are based on the properties of microscopic "p-n junctions" and Dember cells, respectively. In the first of these models, the large photovoltages are said to arise as the result of summing elementary photovoltages generated at internal barriers or junctions which may be Schottky barriers[53] or barriers due to surface states[42] or grain boundaries.[16,40,54] These various models are commonly referred to simply as p-n-junction models.[27] According to these models, each junction may be expected to generate a photovoltage given by[27]

$$V_{p\text{-}n} = (kT/e)\ln(1 + I_{sc}/I_{rs}) , \tag{28}$$

where I_{sc} is the short-circuit photocurrent and I_{rs} the reverse-bias saturation current for the junction. Various combinations of junctions, photoshunts, and bridges located at different depths have been proposed[31,51] to account for the complex spectral sensitivity which some of the films display.

The second type of model which has been suggested is based on the Dember effect in oriented microcrystals.[17,18,27,38,48] According to this model, each oriented Dember cell generates a photovoltage which may be expressed as[27]

$$V_D = V_d - V_i = (kT/e)\,[(1-b)/(1+b)]\ln(\sigma_i/\sigma_d) . \tag{29}$$

In the above expression, b is the ratio of electron to hole mobility and the subscripts i and d refer to parameters evaluated at the illuminated and dark surfaces, respectively. It has been proposed[38,39] that surface recombination effects which lead to "anomalous" photogenerated carrier distributions may be responsible for the photovoltaic polarity and spectral sensitivity which various films exhibit.

We would like to suggest a new model for these photovoltaic films which is based on the properties of an anisotropic relaxation semiconductor. Zhadko and Romanov have earlier suggested[43] that anisotropic diffusion may be the source of the anomalous photovoltages which the obliquely deposited films display. In addition, Uskov and Petrov[22] have explained certain aspects of the effect in PbI_2 films in a qualitative way on the basis of this mechanism and Genzow[44] has attributed the photovoltaic effect in obliquely deposited Te films to the natural anisotropy of this semiconductor. The model we suggest combines the mechanism of anisotropic diffusion with the properties of the relaxation semiconductor to obtain a theory which accounts for the various aspects of observed behavior.

B. Isojunction model

The photovoltaic films are relaxation semiconductors. The relaxation case may be expected whenever sufficiently short carrier lifetimes occur in conjunction with sufficiently high resistivity. In disordered materials containing appreciable densities of localized electronic states, it tends to be self-realizing: With large concentrations of equality centers present, carrier capture times are typically short and most of the carriers, at a given instant, are localized at these centers. This leads to high resistivity which, in turn, increases the effectiveness of the now unscreened equality centers.[2,5] With high resistivity, dielectric relaxation times are necessarily long. For a dielectric constant of 12, the dielectric relaxation time in seconds is approximately 10^{-12} times the resistivity in Ω cm. The photovoltaic films, which have resistivities $\sim 10^6$–10^{11} Ω cm, are certainly relaxation semiconductors and must be analyzed as such.

All of the films that exhibit large photovoltages are grown in a peculiar way: An oblique-vapor-deposition process is employed. X-ray diffraction studies[45,46,52] have revealed how this process affects film growth. In these studies, crystal growth patterns of CdTe films prepared with the vapor beam normal to the substrate were compared with those grown using the oblique deposition technique. Both types of films were found to be polycrystalline, with the crystallites preferentially oriented. The normal deposition produced small crystals with (111) planes parallel to the substrate surface, whereas the oblique deposition produced "remarkable oriented growth"[46] with crystal (111) planes inclined toward the vapor source. This inclination

was found to increase gradually with film thickness. A mixed cubic-hexagonal phase was also detected in some of the films.[46] Recent electron-micrographic studies[47] of obliquely deposited CdTe confirm the above observations. As has been mentioned in Sec. II A, this is exactly the type of crystal growth needed to produce an anisotropic relaxation semiconductor. On the basis of this evidence, the generalization we make is that *all* of the obliquely deposited photovoltaic films are like these.

The photovoltaic films are thus envisioned to be composed of thousands of anisotropic crystals which are the result of the oblique-deposition process. Crystals within a given film will generally be characterized by different depth-dependent anisotropy factors of a form determined by how each individual crystal has grown. These films can, however, be analyzed in a simple way by assigning some average anisotropy factor to each. Such an approach would seem appropriate since, with thousands of crystals present in a single film, good statistics will prevail and effects at the crystal boundaries tend to cancel in any case. This is the approach that will be employed.

A large majority[55] of the photovoltaic films exhibit the following properties: (a) high resistivity, [14–25] (b) short-circuit current directly proportional to illumination intensity, [16,18,20,22,25] (c) photovoltage directly proportional to film length, [16,17,24,25] (d) photovoltage directly proportional to light intensity followed by saturation at high illumination levels, [17–22,25] (e) complex photovoltaic spectra, [19–26,30] (f) asymmetric spectra when illuminated through the substrate.[22,25,30,38] These are the properties of an anisotropic trap-dominated relaxation semiconductor. To illustrate that such is the case, several types of film structures will be described in some detail.

First, let us consider a constant-anisotropy film characterized by the parameters listed in

TABLE I. Parameters used to obtain curves shown in Fig. 4.

Parameter	Value
Film thickness y_0	1.0 μm
Dark resistivity ρ_0	2×10^9 Ω cm
Conductivity ratio K	1.0
Anisotropy factor a	0.1
Surface numbers $S_1=S_2$	1.0
Quantum efficiency β	1.0 carrier pairs/photon
Absorption coefficient α	2×10^5 cm^{-1}
Temperature T	300°K

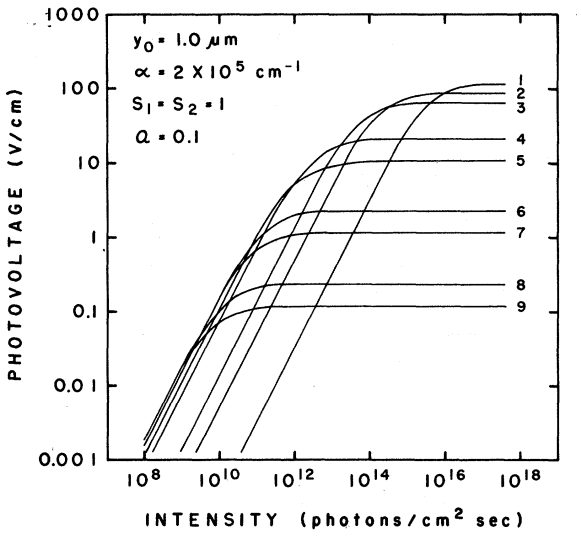

FIG. 4. Photovoltage versus light intensity for constant-anisotropy film described in text when L^* equals (1) 10^{-6}, (2) 5×10^{-6}, (3) 10^{-5}, (4) 5×10^{-5}, (5) 10^{-4}, (6) 5×10^{-4}, (7) 10^{-3}, (8) 5×10^{-3}, (9) 10^{-2} cm.

Table I. The values chosen are thought to be typical of relaxation-case CdTe. A majority of the experimental studies have been concerned with this material. In this case, (15) and (16) apply with J_0^* given by (18). In Fig. 4, computer-generated theoretical plots of the open-circuit photovoltage versus illumination intensity for this type of structure are displayed. The various curves shown were obtained by using different conductivity-locked diffusion lengths ($L^*=10^{-2}$–10^{-6} cm) in the computation of (16). Note, in particular, that the theory predicts large photovoltages in the small-diffusion-length, high-resistivity limit. For large values of L^*, the photoconductivity increases rapidly with illumination intensity, in accord with (19), and V_{oc} quickly saturates. For small values of ρ_0 and L^*, photogenerated electrons and holes make a negligible contribution to the total conductance. In this case, V_{oc} increases linearly with I_0, consistent with (22), and is small in magnitude over the entire range of illumination intensities shown. Thus, the generation of large steady-state[56] photovoltages by an anisotropic semiconductor occurs as an exclusive relaxation-regime effect. The saturation of photovoltages displayed by obliquely deposited CdTe films is observed[34] to occur at illumination levels $I_0\sim10^{16}$–10^{17} photons/cm^2 sec which is consistent with $L^*\sim5\times10^{-6}$–10^{-6} cm for this material. Diffusion lengths of this magnitude imply extremely small excess carrier lifetimes—*a key van Roosbroeck prediction*[2] and one which the present analysis has consistently assumed.

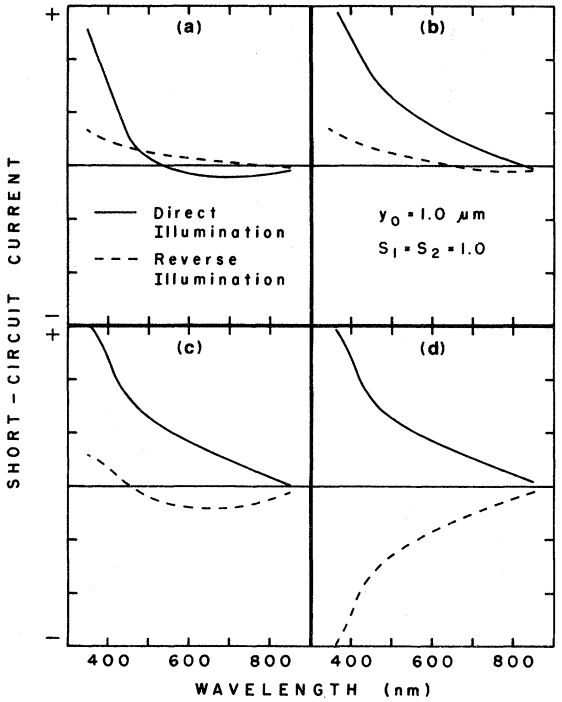

FIG. 5. Spectral distribution of photocurrents generated by 1.0-μm-thick CdTe isojunction with Y_i/Y_0 equal to (a) 0.1, (b) 0.5, (c) 0.8, (d) 1.0. Current scale is 10^{-11} A/division ($I_0 = 10^{16}$ photons/cm^2 sec).

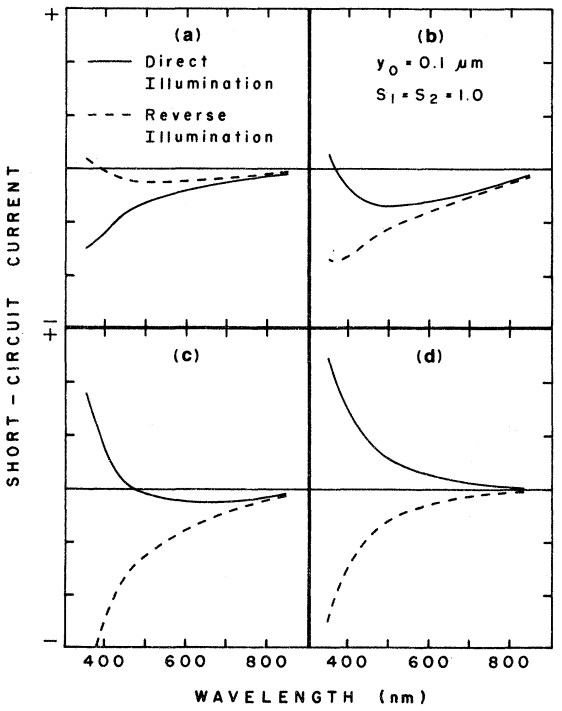

FIG. 6. Photocurrent spectra for 0.1-μm-thick CdTe isojunction with Y_i/Y_0 equal to (a) 0.1, (b) 0.5, (c) 0.8, (d) 1.0. Current scale is 10^{-11} A/division ($I_0 = 10^{16}$ photons/cm^2 sec).

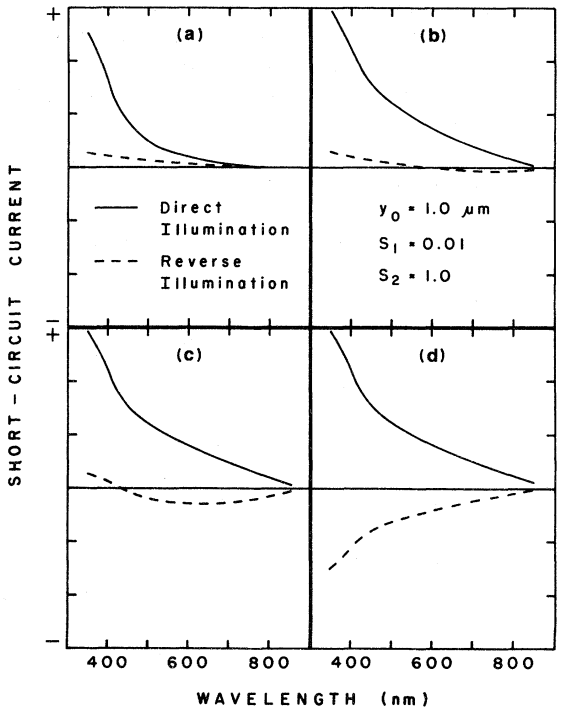

FIG. 7. Photocurrent spectra for 1.0-μm-thick CdTe isojunction for which $S_1 = 0.01$, $S_2 = 1.0$, and Y_0/Y_i equals (a) 0.1, (b) 0.5, (c) 0.8, (d) 1.0. Other parameters are as for Fig. 5. Current scale is 2×10^{-11} A/division ($I_0 = 10^{16}$ photons/cm^2 sec).

The constant-anisotropy structures of Fig. 4 are symmetric and thus produce photovoltages of identical magnitude (but opposite polarity) when the direction of illumination is reversed. More complicated behavior results, however, when this symmetry is absent. This is illustrated by the curves shown in Figs. 5–8 which indicate the spectral characteristics of an abrupt a^+-a^- isojunction. Parameter values (Table II) typical of relaxation-case CdTe were used in (15) and (27) to obtain these curves. Figures 5(a)–5(d) display the spectral distribution of short-circuit currents generated by a 1.0-μm-thick isojunction with Y_i/Y_0 equal to 0.1, 0.5, 0.8, and 1.0, respectively, for cases of direct and reverse (through-the-substrate) illuminations. Note, in particular, that the response of the isojunction is substantially different when the depth of its isoplane is changed and when the direction of illumination is reversed. The photocurrents produced are directly proportional to the light intensity. For $I_0 = 10^{16}$ photons/cm^2 sec, the current scale of Fig. 5 is 10^{-11} A/division. Currents of this magnitude are often observed for obliquely deposited CdTe,[38] and for many of the other photovoltaic films. In Fig. 6, corresponding curves obtained for a thin ($y_0 = 0.1$ μm) isojunction are shown. Other parameters are the

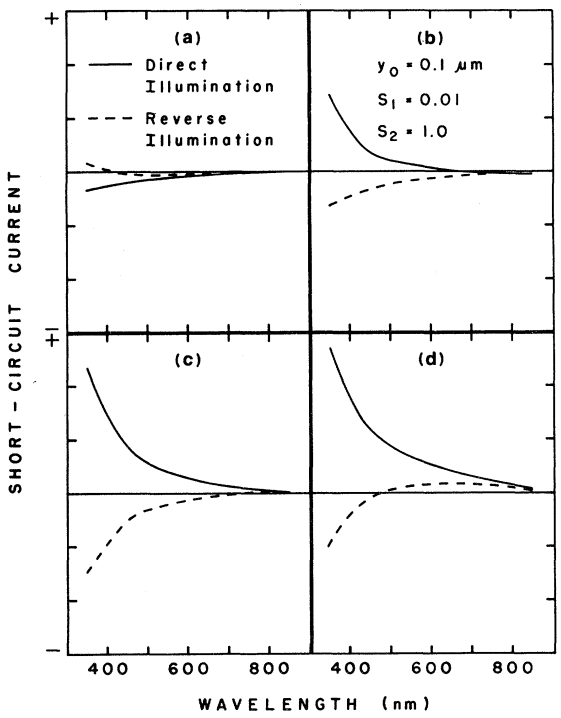

FIG. 8. Spectral distribution of photocurrents for 0.1-μm-thick CdTe isojunction for which $S_1 = 0.01$, $S_2 = 1.0$, and Y_i/Y_0 equals (a) 0.1, (b) 0.5, (c) 0.8, (d) 1.0. Other parameters are as for Fig. 6. Current scale is 2×10^{-11} A/division ($I_0 = 10^{16}$ photons/cm^2 sec).

same as for Fig. 5. Note the differences in the spectra shown in these two figures.

The properties of the isojunction also depend on the nature of its surfaces. The asymmetry of this structure is enhanced when its surface numbers are not equal. This is illustrated by the curves shown in Figs. 7 and 8 for which $S_1 = 0.01$ and $S_2 = 1.0$. Other parameters are the same as for Figs. 5 and 6, respectively. For $I_0 = 10^{16}$ photons/cm^2 sec, the current scale is 2×10^{-11} A/division. Surface effects are expected to be more important for thin specimens and a comparison of the spectra of Fig. 6 and Fig. 8 shows this to be the case. For these 0.1-μm-thick structures, surface recombination actually plays a dominant role in determining the distribution of photogenerated carriers within the material in accord with (11). This is illustrated by the behavior of the constant-anisotropy structures of Fig. 6(d) and Fig. 8(d). With $S_1 = 0.01$, the film of Fig. 8(d) generates positive-polarity photocurrents over most of the visible spectrum irrespective of the direction of illumination.

The saturated photovoltages ($I_0 > 10^{17}$ photons/cm^2 sec) generated by the sixteen isostructures of Figs. 5–8, upon exposure to light of selected wavelengths, are listed in Table III. Parameter values of Table II together with (16) were used in the calculations. Note, in particular, that large photovoltages result even for the relatively small[58] anisotropy factors, $a^+ = 0.05$, $a^- = -0.01$, employed. These anisotropy factors correspond to diffusion of electrons and holes at angles which differ by about 2.5° and 0.5°, respectively, in the two separate regions of the isojunction.

The analysis of more complicated specimens, such as an a^+-a^--a^+ double isostructure, is entirely straightforward but will not be included here. The properties displayed by the simple structures discussed above illustrate the point we wish to make: A wide variety of behavior is to be expected of the obliquely deposited films. Changes in growth parameters such as deposition angle, deposition rate, source and substrate temperatures, substrate material, chamber pressure, and ambient impurities will all affect the isostructure of the crystals formed and thus the photovoltaic properties of a given film. An exact duplication of the growth techniques and subsequent handling may be necessary to produce films which display reproducible properties. Twenty-odd years of observations, however, suggest that this is virtually impossible: Many of the obliquely deposited photovoltaic films are essentially unique.

A "remarkable correlation"[27] between the photovoltage and dark resistance of films of different semiconductors illuminated at constant light intensity has been observed. This aspect of behavior is illustrated in Fig. 9 for Ge,[18] Si,[27] and CdTe.[16] Each set of data shown was obtained by measuring the photovoltage and resistance of an individual film at several temperatures. These observations suggest that a single mechanism is responsible for the photovoltaic properties of these different materials. None of the current theories have been

TABLE II. Parameters used to obtain curves shown in Figs. 5–8.

Parameter	Value
Dark resistivity ρ_0	2×10^9 Ω cm
Conductivity ratio K	1.0
Diffusion length L	2×10^{-6} cm
Anisotropy factors:	
a^+	0.05
a^-	−0.01
Quantum efficiency β	1.0 carrier pairs/photon
Absorption coefficient α	Values[a] for CdTe
Temperature T	300 °K

[a]Reference 34.

TABLE III. Saturated photovoltages ($I_0 > 10^{17}$ photons/cm^2 sec) generated by the isostructures of Figs. 5–8. Values in parentheses are for reverse (through-the-substrate) illumination.

	Photovoltage (V/cm)				
Isostructure Fig. No.	$\lambda = 400$ nm $\alpha = 2\times10^5$ cm^{-2}	$\lambda = 500$ nm $\alpha = 9\times10^4$ cm^{-1}	$\lambda = 600$ nm $\alpha = 6\times10^4$ cm^{-1}	$\lambda = 700$ nm $\alpha = 3.5\times10^4$ cm^{-1}	$\lambda = 800$ nm $\alpha = 1.7\times10^4$ cm^{-1}
5(a)	26 (11)	−4.7 (5.3)	−8.8 (3.5)	−9.0 (1.4)	−6.9 (−0.9)
5(b)	54 (11)	26 (4.5)	16 (1.2)	6.3 (−2.4)	−1.5 (−4.4)
5(c)	54 (6.8)	26 (−7.5)	18 (−11)	9.6 (−12)	2.7 (−9.1)
5(d)	54 (−54)	27 (−27)	18 (−18)	11 (−11)	5.3 (−5.3)
6(a)	−35 (−2.1)	−27 (−11)	−24 (−14)	−22 (−16)	−20 (−17)
6(b)	−11 (−49)	−30 (−47)	−24 (−46)	−37 (−44)	−39 (−42)
6(c)	25 (−78)	−5.2 (−53)	−14 (−46)	−20 (−39)	−25 (−34)
6(d)	47 (−47)	22 (−22)	15 (−15)	8.6 (−8.6)	4.2 (−4.2)
7(a)	67 (15)	20 (5.3)	8.4 (3.6)	1.8 (1.8)	−0.5 (0.3)
7(b)	92 (11)	48 (4.5)	32 (1.3)	17 (−2.0)	6.2 (−3.1)
7(c)	92 (6.8)	48 (−7.5)	34 (−11)	20 (−11)	9.0 (−7.8)
7(d)	92 (−54)	49 (−27)	34 (−18)	21 (−10)	12 (−4.1)
8(a)	−14 (3.1)	−11 (−2.8)	−9.8 (−4.3)	−8.8 (−5.5)	−8.0 (−6.4)
8(b)	40 (−30)	14 (−19)	7.3 (−15)	2.1 (−11)	−1.5 (−7.8)
8(c)	74 (−55)	38 (−23)	28 (−13)	20 (−4.4)	13 (1.7)
8(d)	94 (−26)	62 (6.6)	53 (16)	46 (24)	40 (29)

able to account for this simple aspect of behavior. Here, an explanation is given: All of the films are anisotropic relaxation semiconductors. Some may be isojunctions or generalizations thereof. For illumination levels which lead to small conductivity modulation, (22) applies and predicts the observed correspondence between photovoltage and dark resistance, provided I_{sc} is temperature insensitive. This is the observed behavior[16,17] of this parameter in these materials.

The ultimate state of a strongly trap-dominated relaxation semiconductor is the $K = 1$ or minimum conductivity state for which

$$\sigma_{min} = 2n_i e(\mu_p \mu_n)^{1/2}, \tag{30}$$

where n_i is the intrinsic carrier concentration at a given temperature. With mobilities and diffusion lengths expected[2] to be small and about equal in all such materials, the new theory predicts saturation of V_{oc} to occur at illumination levels which vary in reverse order of band-gap energy in this limit. This is the observed[19] saturation order for CdTe, GaAs, Si, and Ge at room temperature. For a given semiconductor, the theory also predicts saturation in V_{oc} at smaller light intensities as the temperature is decreased. This is observed[16,27] to be the case.

Relaxation-case semiconductors characterized by appreciable *Hall mobilities* can exhibit a giant photomagnetoelectric (PME) effect. CdTe appears to be one such material. PME photovoltages as large as 70 V have been reported[33] for obliquely deposited films of this semiconductor at large applied magnetic fields. Fig. 10 shows the spectral distribution of photocurrents exhibited by three such films. In Fig. 10(a) the "anomalous" short-circuit current I_{sc} displayed by these films in the absence of a magnetic field is shown. The corresponding photomagnetoelectric contribution I_{PME}, obtained with the films in a transverse magnetic field by substracting away the anomalous photocurrent, is shown in Fig. 10(b). None of the current theories[33,34,37,38] can account for these observations in a self-consistent way. Here, an explanation is given: The films are anisotropic relaxation semiconductors with dissimilar isostructures, as is evidenced by the different spectra of Fig. 10(a). An applied magnetic field introduces

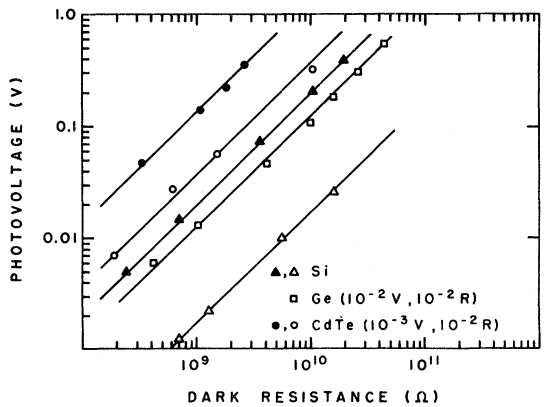

FIG. 9. Photovoltage versus dark resistance reported for Si (Ref. 27), Ge (Ref. 18), and CdTe (Ref. 16).

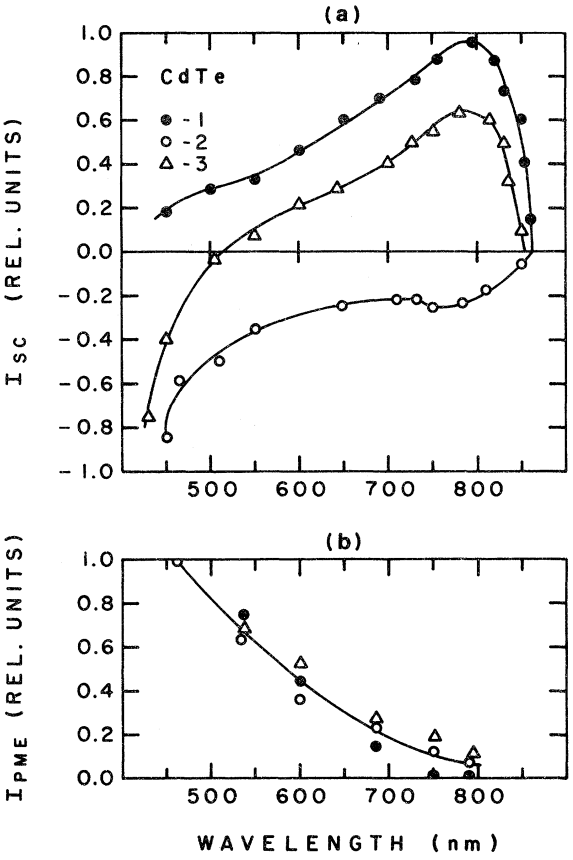

FIG. 10. Spectral distribution of photocurrents generated by three CdTe films (Ref. 33): (a) "anomalous" contribution, (b) photomagnetoelectric contribution.

an additional uniform anisotropy. To first order in anisotropy factors the effects add, in which case

$$I_{tot} = I_{sc} + I_{PME}\,, \tag{31}$$

$$V_{tot} = V_{oc} + V_{PME}\,, \tag{32}$$

where I_{PME} and V_{PME} are given by (15) and (16), respectively. In these expressions, $J^* = aJ_0^*$ where a is a magnetic anisotropy factor or Hall angle,[7,10] that is, $a = \theta_p + |\theta_n|$, where θ_p and θ_n are Hall angles for holes and electrons, respectively. For relatively thick films and whenever $S_1 \leqq S_2$, the present theory thus predicts monotonic spectra of the type displayed in Figs. 5(d)–8(d), which accounts for the observations shown in Fig. 10(b) for direct illumination.

The new theory is also in accord with other observed[33] characteristics of the PME effect in this semiconductor, including the linear dependence of I_{PME} on light intensity; the linear variation of V_{PME} with magnetic field strength, which implies small Hall angles and justifies the use of (31) and (32); the saturation of V_{oc} and V_{PME} at *identical* illumination levels. For thin specimens and whenever $S_1 < S_2$, (15) predicts I_{PME} spectra of the type shown in Fig. 8(d), which accounts for the recently reported[34] spectra obtained for this type of sample under direct and reverse (through-the-substrate) illuminations. The condition $S_1 < S_2$ is here attributed to an anneal of the isostructure which produces a free surface (away from the substrate) that is actually more ordered than the bulk.

Such annealing effects together with the incorporation of impurities within the isostructure are, perhaps, responsible for the changes in photovoltaic properties[16,18] which some of the obliquely deposited films display over extended time periods. The incorporation of impurities such as ambient gases may be expected to increase the density of localized states which serve as equality centers in the recombination processes. The dramatic increase in resistance[18] exhibited by certain Ge films upon exposure to O_2 is, in fact, an external signal of an internal transformation of these samples to a state deep within the relaxation regime.

Models based on the Dember mechanism lose much of their appeal when the photovoltaic films are recognized to be relaxation semiconductors. Such models lead to predictions which are in direct conflict with observations and cannot, in principle, apply. The familiar expression (29) for the Dember effect is derived under the assumption of excess carrier neutrality ($\delta n = \delta p$) and is only valid for lifetime semiconductors which exhibit negligible trapping. The correct expression for a conductivity-locked relaxation semiconductor is given by[7]

$$V_D = (kT/e)[(1-K)/(1+K)]\ln[G^*(0)/G^*(Y_0)]\,, \tag{33}$$

where

$$G_0^*(Y) = g_0 + [\alpha\beta I_0/(1-A^2)](C_1 e^{-Y} + C_2 e^{Y} + e^{-AY}) \tag{34}$$

is the net rate at which mobile-carrier-space charge is generated at the respective surfaces, with g_0 the thermal-equilibrium generation rate. Now, the ultimate state of a strongly trap-dominated relaxation semiconductor is the $K = 1$ or minimum conductivity state, for which the Dember effect vanishes. Obliquely deposited films of Ge and Si, two materials for which Dember models have been suggested,[17,18,29,48] often display resistivities which are equal to and, in some cases, greater than their amorphous counterparts. This suggests that many of the films may be minimum conductivity semiconductors and according to (33) should exhibit no photovoltaic properties. But this is completely contrary to the observations: Films of highest resistivity quite typically display the largest effects. In contrast to this, the theory described here predicts a maximum photovoltage for $K = 1$, other parameters being constant.

The presence of p-n junctions or other types of barriers within the films must also be questioned. Their existence is inferred from a single experimental fact: The obliquely deposited films are highly photovoltaic. However, other aspects of behavior such as asymmetric and nonlinear current-voltage characteristics, metallic-contact effects, or the special dependences of photovoltage and photoconductivity on illumination intensity which are expected for such structures are not observed. Rather, this class of photovoltaic films exhibits high resistivity and *Ohmic conduction* at low and moderate applied fields independent of the contact electrodes.[16,17,19,21,22,25,26] This is the expected[2] behavior for a trap-dominated relaxation semiconductor. A number of p-n-junction models have been proposed[16,29,31,32,42] to account for the photovoltaic properties of CdTe films. However, none of these models can explain the various observed properties of this semiconductor in a self-consistent way.[36,37,38,43] Nor can such models account for the recently observed[60,61] switching effect in this material. These recent experiments, performed on polycrystalline CdTe "sandwiches," have disclosed aspects of transport in one-to-one correspondence with certain amorphous alloys. In particular, preswitching I-V characteristics identical with those of the alloys were observed. This preswitching behavior in the alloys is accounted for[2] on the basis of a field-assisted activation of carriers, in which electron and hole conductivities remain equal as they are increased. This is an example of conductivity-locked behavior for $K=1$.

IV. SUMMARY

A simple approach is used to analyze the photovoltaic properties of anisotropic relaxation semiconductors. The characteristics of a new photovoltaic structure, an isojunction, emerge from this analysis. A new theory for the larger-than-band-gap photovoltages exhibited by many obliquely deposited semiconducting films is proposed. The theory accounts for the various aspects of observed behavior in a self-consistent manner.

[1]W. van Roosbroeck, Phys. Rev. 123, 474 (1961).
[2]W. van Roosbroeck, J. Non-Cryst. Solids 12, 232 (1973).
[3]W. van Roosbroeck and H. C. Casey, Jr., in *Proceedings of the Tenth International Conference of the Physics of Semiconductors* (U. S. AEC, Springfield, Va, 1970), p. 832.
[4]H. J. Queisser, H. C. Casey, Jr., and W. van Roosbroeck, Phys. Rev. Lett. 26, 551 (1971).
[5]W. van Roosbroeck and H. C. Casey, Jr., Phys. Rev. B 5, 2154 (1972).
[6]C. Popescu and H. K. Henisch, Phys. Rev. B 11, 1563 (1975).
[7]J. F. Schetzina, Phys. Rev. B 11, 4994 (1975).
[8]W. van Roosbroeck and W. G. Pfann, J. Appl. Phys. 33, 2304 (1962).
[9]R. M. Shah and J. F. Schetzina, Phys. Rev. B 5, 4014 (1972).
[10]A. Subramanian, S. J. Gordon, and J. F. Schetzina, Phys. Rev. B 9, 536 (1974).
[11]A. Rose, Phys. Rev. 97, 322 (1955).
[12]S. M. Ryvkin, *Photoelectric Effects in Semiconductors* (Consultants Bureau, New York, 1964), p. 116ff.
[13]W. van Roosbroeck, Phys. Rev. 101, 1713 (1956).
[14]L. Pensak, Phys. Rev. 109, 601 (1958).
[15]B. Goldstein, Phys. Rev. 109, 601 (1958).
[16]B. Goldstein and L. Pensak, J. Appl. Phys. 30, 155 (1959).
[17]H. Kallmann, B. Kramer, and E. Haidemenakis, J. Electrochem. Soc. 108, 247 (1961).
[18]H. Kallmann, G. Marmor Spruch, and S. Trester, J. Appl. Phys. 43, 469 (1972).
[19]E. I. Adirovich, V. M. Rubinov, V. M. Rubinov, and Yu. M. Yuabov, Fiz. Tverd. Tela 6, 3180 (1964) [Sov. Phys.-Solid State 6, 2540 (1965)].
[20]E. I. Adirovich, V. F. Roslyakova, and Yu. M. Yuabov, Fiz. Tekh. Poluprovoda 2, 1020 (1968) [Sov. Phys.-Semicond. 2, 848 (1968) [Sov. Phys.-Semicond. 2, 848 (1969)].
[21]V. A. Ignatyuk and F. T. Novik, Fiz. Tekh. Poluprovoda 4, 472 (1970) [Sov. Phys.-Semicond. 4, 394 (1970)].
[22]E. M. Uskov and V. P. Petrov, Fiz. Tekh. Poluprovodn. 5, 2204 (1971) [Sov. Phys.-Semicond. 5, 1920 (1972)].
[23]I. A. Karpovich and M. V. Shilova, Fiz. Tverd. Tela 5, 3560 (1963) [Sov. Phys.-Solid State 5, 2612 (1964)].
[24]V. M. Lyubin and G. A. Fedorova, Dokl. Akad. Nauk SSSR 135, 833 (1960) [Sov. Phys.-Dokl. 5, 1343 (1960)].
[25]V. M. Lyubin and G. A. Fedorova, Fiz. Tverd. Tela 4, 2026 (1962) [Sov. Phys.-Solid State 4, 1486 (1963)].
[26]E. I. Adirovich and Yu. M. Yuabov, Dokl. Akad. Nauk SSSR 155, 1286 (1964) [Sov. Phys.-Dokl. 9, 296 (1964)].
[27]H. W. Brandhorst, Jr., and A. E. Potter, Jr., J. Appl. Phys. 35, 1997 (1964).
[28]E. I. Adirovich, V. M. Rubinov, and Yu. M. Yuabov, Dokl. Akad. Nauk SSSR 164, 529 (1965) [Sov. Phys.-Dokl. 10, 844 (1966)].
[29]E. I. Adirovich, V. M. Rubinov, and Yu. M. Yuabov, Dokl. Akad. Nauk SSSR 168, 1037 (1966) [Sov. Phys.-Dokl. 11, 521 (1966)].
[30]E. I. Adirovich, V. M. Rubinov, and Yu. M. Yuabov, Dokl. Akad. Nauk SSSR 174, 545 (1967) [Sov. Phys.-Dokl. 12, 477 (1967)].
[31]E. I. Adirovich, V. A. Benderskii, and N. Shakirov, Dokl. Akad. Nauk SSSR 181, 1090 (1968) [Sov. Phys.-Dokl. 13, 779 (1969)].
[32]E. I. Adirovich, E. M. Mastov, and Yu. M. Yuabov, Dokl. Akad. Nauk SSSR 188, 1254 (1969) [Sov. Phys.-Dokl. 14, 994 (1970)].
[33]E. I. Adirovich, E. M. Mastov, and Yu. M. Yuabov, Fiz. Tekh. Poluprovodn. 5, 1415 (1971) [Sov. Phys.-Semicond. 5, 1241 (1972)].
[34]E. I. Adirovich, D. A. Aronov, E. M. Mastov, and Yu. M. Yuabov, Fiz. Tekh. Poluprovodn. 8, 354 (1974) [Sov. Phys.-Semicond. 8, 226 (1974)].
[35]M. I. Korsunskii, M. M. Sominskii, and B. A. Zubarev, Dokl. Akad. Nauk SSSR 180, 66 (1968) [Sov. Phys.-

Dokl. 13, 420 (1968)].
[36]M. I. Korsunskii, M. M. Sominskii, and B. A. Zubarev, Dokl. Akad. Nauk SSSR 180, 319 (1968) [Sov. Phys.-Dokl. 13, 437 (1968)].
[37]M. I. Korsunskii, M. M. Sominskii, and V. M. Smurygin, Dokl. Akad. Nauk SSSR 203, 332 (1972) [Sov. Phys.-Dokl. 17, 268 (1972)].
[38]M. I. Korsunskii and M. M. Sominskii, Fiz. Tekh. Poluprovodn. 7, 480 (1973) [Sov. Phys.-Semicond. 7, 342 (1973)].
[39]H. Onishi, S. Kurokawa, and K. Ieyasu, J. Appl. Phys. 45, 3205 (1974).
[40]F. T. Novik, Fiz. Tverd. Tela 5, 3142 (1963) [Sov. Phys.-Solid State 5, 2300 (1964)].
[41]I. P. Kretsu, N. K. Malkoch, M. P. Razloga, and A. G. Cheban, Fiz. Tekh. Poluprovodn. 8, 1198 (1974) [Sov. Phys.-Semicond. 8, 777 (1974)].
[42]R. H. Williams and H. R. Johnson, Solid State Commun. 16, 873 (1975).
[43]I. P. Zhadko and V. A. Romanov, Phys. Status Solidi 28, 797 (1968).
[44]D. Genzow, Phys. Status Solidi A 7, K77 (1971).
[45]M. Kamiyama, M. Haradome, and H. Kukimoto, Jpn; J. Appl. Phys. 1, 202 (1962).
[46]J. Matsuno and M. Inoue, Jpn. J. Appl. Phys. 6, 297 (1967).
[47]N. Dhere, R. Pinheiro, and N. R. Parikh, J. Vac. Sci. Technol. 11, 599 (1974).
[48]M. Takahashi, F. Kou, and O. Tada, Jpn. J. Appl. Phys. 7, 1446 (1968).
[49]P. P. Konorov and K. Liubits, Fiz. Tverd. Tela 6, 71 (1963) [Sov. Phys.-Solid State 6, 55 (1964)].
[50]P. P. Konorov, Fiz. Tekh. Poluprovodn. 2, 1724 (1968) [Sov. Phys.-Semicond. 2, 1437 (1969)].
[51]W. Ma, R. M. Anderson, and S. J. Hruska, J. Appl. Phys. 46, 2650 (1975).
[52]R. L. Holden, M. S. thesis (North Carolina State University, 1975) (unpublished).
[53]J. I. Pankove, *Optical Process in Semiconductors* (Prentice-Hall, Englewood Cliffs, N. J., 1971), Chap. 14.
[54]A. R. Hutson, Bull. Am. Phys. Soc. 6, 110 (1961).
[55]Some of the films do not exhibit all of the properties listed, particularly at high illumination levels. Nontypical behavior in some polycrystalline specimens which lack the degree of disorder of the amorphous state is to be expected however, and is attributed to an insufficient density of equality centers in these samples. Under such conditions, carrier transport is generally *not* conductivity locked and is governed by nonlinear differential equations (see Ref. 7). Detailed treatment of this case is beyond the present scope.
[56]The production of larger-than-band-gap photovoltages is not a unique property of anisotropic relaxation semiconductors, however. In recent experiments in which specially oriented and compressed intrinsic (lifetime-case) Ge single crystals were used, larger-than-band-gap photovoltages were observed when the specimens were exposed to high-intensity short light pulses. See Refs. 10 and 57 for a detailed discussion.
[57]S. J. Gordon and J. F. Schetzina, Bull. Am. Phys. Soc. 19, 323 (1974).
[58]Anisotropy factors as large as 0.5 have been generated in compressed Ge specimens. See Refs. 10, 57, and 59.
[59]T. S. Hahn and J. F. Schetzina, Phys. Rev. B 7, 729 (1973).
[60]G. M. Friedman, G. A. Denton, and J. F. Schetzina, Bull. Am. Phys. Soc. 19, 1117 (1974).
[61]G. A. Denton, G. M. Friedman, and J. F. Schetzina, J. Appl. Phys. 46, 3044 (1975).